Nogo-A is a negative regulator of CNS angiogenesis

Thomas Wälchli[a,b,c,1], Vincent Pernet[a,b,1], Oliver Weinmann[a,b], Jau-Ye Shiu[d], Anna Guzik-Kornacka[a,b], Guillaume Decrey[c], Deniz Yüksel[e,f], Hannah Schneider[c], Johannes Vogel[g], Donald E. Ingber[e,f,h], Viola Vogel[d], Karl Frei[c], and Martin E. Schwab[a,b,2]

[a]Brain Research Institute, University of Zurich, CH-8057 Zurich, Switzerland; [b]Department of Health Sciences and Technology, Swiss Federal Institute of Technology Zurich, CH-8057 Zurich, Switzerland; [c]Department of Neurosurgery, University Hospital Zurich, CH-8091 Zurich, Switzerland; [d]Laboratory of Applied Mechanobiology, Department of Health Sciences and Technology, Swiss Federal Institute of Technology Zurich, CH-8093 Zurich, Switzerland; [e]Wyss Institute for Biologically Inspired Engineering at Harvard University, Boston, MA 02115; [f]Vascular Biology Program, Departments of Pathology and Surgery, Children's Hospital and Harvard Medical School, Boston, MA 02115; [g]Institute of Veterinary Physiology, Vetsuisse Faculty, University of Zurich, CH-8057 Zurich, Switzerland; [h]Department of Bioengineering, Harvard School of Engineering and Applied Sciences, Cambridge, MA 02138

Edited by Dean Li, University of Utah, Salt Lake City, UT and accepted by the Editorial Board March 1, 2013 (received for review September 24, 2012)

Nogo-A is an important axonal growth inhibitor in the adult and developing CNS. In vitro, Nogo-A has been shown to inhibit migration and cell spreading of neuronal and nonneuronal cell types. Here, we studied in vivo and in vitro effects of Nogo-A on vascular endothelial cells during angiogenesis of the early postnatal brain and retina in which Nogo-A is expressed by many types of neurons. Genetic ablation or virus-mediated knock down of Nogo-A or neutralization of Nogo-A with an antibody caused a marked increase in the blood vessel density in vivo. In culture, Nogo-A inhibited spreading, migration, and sprouting of primary brain microvascular endothelial cells (MVECs) in a dose-dependent manner and induced the retraction of MVEC lamellipodia and filopodia. Mechanistically, we show that only the Nogo-A–specific Delta 20 domain exerts inhibitory effects on MVECs, but the Nogo-66 fragment, an inhibitory domain common to Nogo-A, -B, and -C, does not. Furthermore, the action of Nogo-A Delta 20 on MVECs required the intracellular activation of the Ras homolog gene family, member A (Rho-A)-associated, coiled-coil containing protein kinase (ROCK)-Myosin II pathway. The inhibitory effects of early postnatal brain membranes or cultured neurons on MVECs were relieved significantly by anti–Nogo-A antibodies. These findings identify Nogo-A as an important negative regulator of developmental angiogenesis in the CNS. They may have important implications in CNS pathologies involving angiogenesis such as stroke, brain tumors, and retinopathies.

developmental neuroscience | endothelial tip cells | neurovascular link

In many organs, the vascular and the innervation pattern show remarkable similarities (1, 2). To find their appropriate targets, developing nerves and blood vessels possess specialized structures at their leading edge: endothelial tip cells (3, 4) and axonal growth cones. Their filopodial extensions sense specific guidance cues and steer the migrating cell or growing fiber (5). There is increasing evidence that attractive and repulsive molecular guidance cues are shared between capillary endothelial tip cells and neuronal growth cones; several axon guidance molecules and their receptors have been shown also to guide growing blood vessels and to be essential for normal vascular patterning (1, 2).

Nogo-A is a high-molecular-weight membrane protein expressed on the surface of oligodendrocytes and neurons that acts as a growth inhibitory, antiadhesive, and growth cone-collapsing factor (6–8). In addition, Nogo-A exerts repulsive and guidance functions for growing neurites during development (9), influences the migration of cells in the early neural tube (10, 11), and is an important restricting factor for axonal regeneration and plasticity in the adult CNS (12). Nogo-B is a short isoform of Nogo more widely expressed in the body (13). Its roles for neurite growth are unclear, but Nogo-B has been shown to influence vascular remodeling after lesions in peripheral blood vessels by enhancing the migration of endothelial cells and by repelling vascular smooth muscle cells (14–16). In the zebrafish, Nogo-B and its specific receptor NgBR have proangiogenic effects (17). So far, the role of Nogo proteins in angiogenesis of the CNS has not been investigated, and the role of Nogo-A on vascular endothelial cells is completely unknown. Here, using a variety of in vivo and in vitro assays, we show that Nogo-A and its specific inhibitory domain Nogo-A Delta 20 is a negative regulator of angiogenesis in the CNS of mammals.

Results

Developmental CNS Angiogenesis Occurs Postnatally in a Nogo-A–Rich Environment. The brain is vascularized predominantly by sprouting angiogenesis (18) starting from the surrounding perineural vascular plexus in the meninges. After embryonic formation of the big penetrating vessels, capillarization of the brain parenchyma occurs mainly postnatally and is highly dynamic (19). In postnatal day 4 (P4) and P8 forebrain cortices, hippocampi, corpora callosa, and superior colliculi, Nogo-A was widely expressed in the tissue through which isolectin B4 $(IB4)^+$ blood vessels were growing (Fig. 1 *A* and *B*). βIII-tubulin and Nogo-A colocalized in neuronal cells (Fig. S1*A*), and Nogo-A was expressed in neuronal nuclear antigen $(NeuN)^+$ neurons (Fig. S1*B*) but was absent in endothelial cells labeled with IB4 or the endothelial-specific marker glucose transporter 1 (GLUT-1) (Fig. 1*C* and Fig. S1*C*). Moreover, Nogo-A was undetectable in P8 primary brain-derived microvascular endothelial cells (MVECs) by Western blot analysis (Fig. 1*D*). Glial fibrillary acidic protein $(GFAP)^+$ astrocytes showed no Nogo-A expression, and oligodendrocytes start developing only at this stage of development (20). Thus, we conclude that vascular endothelial cells and in particular their growing tips in the postnatal brain have a high chance of encountering Nogo-A–expressing neurons.

IB4-labeled endothelial tip cells with their typical protruding filopodia could be recognized in P4 and P8 brain sections. These capillary tip cells and their filopodia were surrounded by Nogo-A–expressing neurons identified by βIII-tubulin staining (Fig. 1*E* and Fig. S1*A*), as was particularly evident in confocal 3D projections which showed the close spatial relationship between Nogo-A in the neuropil and angiogenic tip cell filopodia (Fig. 1*F*). Nogo-A could not be detected in Nogo-$A^{-/-}$ animals, thus confirming the specificity of the Nogo-A immunostaining (Fig. S1*E*), as previously described (21).

Mature CNS endothelial cells are surrounded by perivascular supportive cells such as pericytes and astrocytes, which contribute to the neurovascular unit (22–24). In the developing brain, platelet derived growth factor receptor β $(PDGFR\beta)^+$ pericytes partially colocalized with the endothelium, excluding tip cell filopodia (Fig. 1 *G* and *H*). Furthermore, $GFAP^+$ astrocytic processes formed a typical pattern for this postnatal stage, but tip

Author contributions: T.W., V.P., O.W., D.E.I., V.V., K.F., and M.E.S. designed research; T.W., V.P., O.W., J.-Y.S., A.G.-K., G.D., D.Y., H.S., J.V., and K.F. performed research; T.W., O.W., J.-Y.S., D.Y., J.V., and K.F. analyzed data; and T.W., V.P., and M.E.S. wrote the paper.

The authors declare no conflict of interest.

This article is a PNAS Direct Submission. D.L. is a guest editor invited by the Editorial Board.

[1]T.W.and V.P. contributed equally to this work.

[2]To whom correspondence should be addressed. E-mail: schwab@hifo.uzh.ch.

See Author Summary on page 8335 (volume 110, number 21).

This article contains supporting information online at www.pnas.org/lookup/suppl/doi:10.1073/pnas.1216203110/-/DCSupplemental.

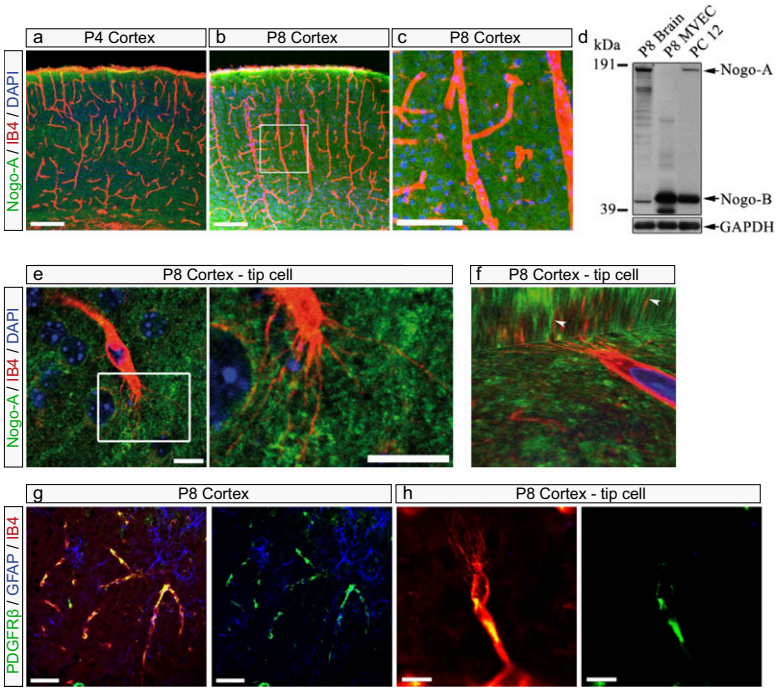

Fig. 1. Blood vessels and their endothelial tip cells grow in Nogo-A–containing tissue in the postnatal brain. Coronal sections (40 μm) of P4 and P8 mouse brains were stained for Nogo-A [Laura antibody (21), green], the vascular endothelial cell marker IB4 (red), and the general nuclear marker DAPI (blue). (*A*–*C*) Blood vessels (red) in the postnatal brain grow in CNS tissue rich in Nogo-A (green) in the cortex at P4 (*A*) and at P8 (*B*). The boxed area in *B* is enlarged in *C*, showing Nogo-A expression (green) in close vicinity of an IB4$^+$ blood vessel (red) in the mouse cortex at P8. Nogo-A was not detectable in IB4$^+$ blood vessels. (*D*) Western blot using a rabbit antiserum recognizing the common N terminus of Nogo-A and Nogo-B [Bianca antibody (21)]. Nogo-A and -B were detected in P8 brain membrane extracts and in PC12 cells but not in P8 brain-derived MVECs. GAPDH was used as loading control (50 μg protein per lane). (*E*) Nogo-A (green) is highly expressed in immediate vicinity of an IB4-labeled endothelial tip cell and its filopodia (red) in a P8 cortex. The boxed area is enlarged at right. (*F*) 3D confocal image *z*-stack projections of a cortical IB4-labeled endothelial tip cell (red) surrounded by Nogo-A (green) in a P8 cortex. Arrowheads indicate IB4$^+$ but Nogo-A$^-$ endothelial tip cell filopodia. (*G* and *H*) Coronal sections (40 μm) of P8 mouse brains were stained for pericytes with anti-PDGFRβ (green), for astrocytes with anti-GFAP (blue), and with the vascular endothelial cell marker IB4 (red). (*G*) PDGFRβ$^+$ pericytes partially cover IB4$^+$ endothelial cells, whereas GFAP$^+$ astrocytes are expressed in the neighborhood of IB4$^+$ endothelial cells. (*H*) In the P8 cortex, PDGFRβ$^+$ pericytes (green) partially surround IB4$^+$ endothelial tip cells (red), excluding filopodial protrusions. (Scale bars: 200 μm in *A* and *B*, 100 μm in *C*, 10 μm in *E*, 50 μm in *G*, and 10 μm in *H*.)

cell filopodia did not follow the astrocytic processes (Fig. 1 *G* and *H*), in contrast to observations in the retina (see below) (25, 26).

These results strongly suggest that endothelial cells of the developing CNS vasculature contact the Nogo-A–containing parenchyma during migration.

Nogo-A Ablation or Neutralization Increases the Blood Vessel Density and the Number of Endothelial Tip Cells in the Postnatal Brain. To determine whether Nogo-A influenced angiogenesis, we investigated the tissue density of IB4$^+$ blood vessels in P8 WT and in P8 Nogo-A$^{-/-}$ mice (27, 28), as well as in P8 WT mice after the i.p. injection of the anti–Nogo-A function-blocking antibody 11C7 raised against 18 amino acids located in the Nogo-A Delta 20 domain (21, 29) or after the injection of an isotype control antibody. Because of the immature, leaky blood–brain barrier in the first postnatal week (30), the antibodies reached the brain tissue in large quantities after i.p. injection (Fig. S2 *A*–*C*). In Nogo-A$^{-/-}$ mice or in mice treated with anti–Nogo-A antibodies, the density of IB4$^+$ blood vessels was increased significantly in all the brain regions analyzed as compared with WT animals or mice injected with a control antibody (Fig. 2 *A*–*H*). Quantitatively, the blood vessel density was increased by 60–100% in the brain areas investigated (Fig. 2 *E*–*H*). The results obtained with the two approaches, i.e., genetic ablation of Nogo-A in knockout mice and the acute application of blocking antibody, were remarkably similar.

To determine whether the additionally formed blood vessels in Nogo-A$^{-/-}$ mice and in mice treated with anti–Nogo-A antibody were functional, perfused vessels, Evans blue was injected intracardially (31), and vessel numbers were quantified using an automated quantification method. The number of perfused vessels increased by 30–60% in all the analyzed P8 CNS regions (Fig. S3 *A*, *C*, *E*, *G*, and *I*). This result indicates that the majority of the supernumerary blood vessels produced by the blockade of Nogo-A are functional and are integrated into the circulation. When IB4$^+$ vessels were counted using the same automated quantification method (showing the number of vessels per square millimeter), the increase was similar to the one obtained with the stereological method (Fig. S3 *B*, *D*, *F*, *H*, and *J*).

Adult Nogo-A$^{-/-}$ mice showed no significant changes in the blood vessel densities in the examined brain areas (Fig. S4), suggesting that the effects of Nogo-A on CNS angiogenesis are compensated mainly at later stages by other regulatory factors of blood vessel formation and stabilization.

Because we observed that Nogo-A was expressed mainly by neurons in early postnatal mouse brains, we wondered if the selective down-regulation of Nogo-A in neurons would affect the blood vessel density at P8. By injecting adeno-associated virus serotype 8 containing shRNA (AAV8.sh–Nogo-A) (32, 33) in the cerebral ventricles at P0, we selectively silenced Nogo-A expression in neurons (Fig. 2*I*). In P8 mice treated with AAV8.sh.RNA–Nogo-A, the density of cortical IB4$^+$ blood vessels was increased by 53% compared with control animals injected with AAV8.GFP control virus (Fig. 2 *J*, *K*, and *L*). This increase in blood vessel density was very similar to those observed in the Nogo-A$^{-/-}$ mice and in mice treated with anti–Nogo-A antibody, indicating that silencing neuronal Nogo-A is sufficient to neutralize the repulsive effects of Nogo-A on blood vessel development.

We analyzed whether inhibiting Nogo-A also affected growing vessel tips, e.g., by an increased number of endothelial tip cells, the motile cells that normally steer blood vessels at their leading edge (Fig. 2*M*). We quantified the number of IB4$^+$ tip cells in the neocortices of P4 and P8 mice. In P4 Nogo-A$^{-/-}$ mice, the number of endothelial tip cells in the cortex was increased by 48% compared with the WT control mice (Fig. 2*N*). At P8, the total number of tip cells per square millimeter was lower than at P4 in both WT and Nogo-A$^{-/-}$ mice, but Nogo-A–deleted animals still showed 91% more tip cells than their WT littermates. Similar results were obtained in the antibody experiments, in which the animals treated with the anti–Nogo-A antibody displayed a 113% increase in the tip cell number as compared with the group treated with the control antibody (Fig. 2*O*).

Together, these results reveal that the chronic ablation of the Nogo-A gene, its antibody-mediated neutralization, or its virus-mediated down-regulation enhances the density of functional CNS blood vessels in the young postnatal brain, at least in part by influencing the formation of tip cells.

Nogo-A Blockade Increases the Blood Vessel Density in the Postnatal Retina. The retina has been used extensively to study angiogenesis in the CNS tissue (26, 34). At P4, βIII-tubulin$^+$ retinal ganglion cells expressed Nogo-A in the vicinity of IB4$^+$ growing

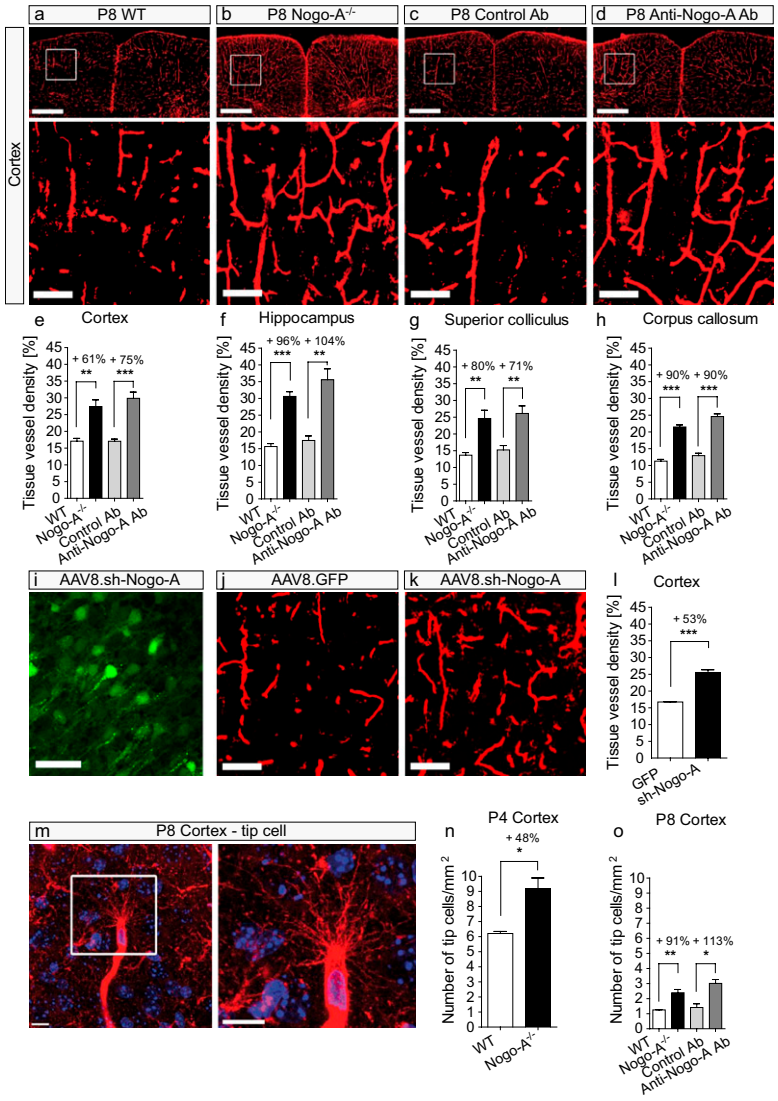

Fig. 2. Genetic deletion of Nogo-A or neutralization by antibodies leads to increased tissue density of blood vessels and to an increased number of cortical endothelial tip cells in the postnatal brain. (*A–D*) Cortices with IB4$^+$ blood vessels in P8 WT mice (*A*), Nogo-A$^{-/-}$ mice (*B*), and mice injected with control antibody (*C*), or with anti–Nogo-A antibody (*D*). Mice without functional Nogo-A (*B* and *D*) showed a higher density of IB4$^+$ vessels than the control animals (*A* and *C*). (*E–H*) Quantification of the tissue density of blood vessels by stereology in P8 cortex (*E*), hippocampus (*F*), superior colliculus (*G*), and corpus callosum (*H*). The tissue vessel density was significantly higher in P8 Nogo-A$^{-/-}$ mice and in P8 WT mice injected with anti–Nogo-A antibody than that in P8 WT mice or in P8 WT mice injected with the isotype control antibody (n = 4). (*I*) GFP-expression (green) in neurons of the cortex of P8 mice injected with AAV8.sh.RNA-Nogo-A-GFP. No Nogo-A down-regulation was observed in the cortex of P8 mice injected with AAV8.sh.RNA-GFP. (*J* and *K*) The density of IB4$^+$ vessels was increased in the cortex of animals injected with AAV8.sh.RNA-Nogo-A-GFP (*K*) as compared with the cortex of control animals injected with AAV8.sh.RNA-GFP (*J*). (*L*) Quantification of the tissue density of blood vessels by stereology in P8 cortex. The tissue vessel density was significantly higher in mice injected with AAV8.sh.RNA-Nogo-A-GFP than in WT mice or mice injected with AAV8.sh.RNA-GFP (n = 3). (*M*) An IB4$^+$ vascular endothelial tip cell in the mouse cortex at P8 (confocal image z-stack maximum intensity projection). Note the numerous filopodial protrusions emerging from the endothelial tip cell body. (*N* and *O*) The number of endothelial tip cells was increased significantly in the cortices of P4 Nogo-A$^{-/-}$ mice (*N*) and of P8 Nogo-A$^{-/-}$ mice and P8 mice injected with anti–Nogo-A (*O*) in comparison with WT mice or mice injected with control antibody (*N* and *O*) (n = 3). All data are shown as mean ± SEM. $*P < 0.05$, $**P < 0.01$, $***P < 0.001$. (Scale bars: 500 μm in *A–D*, *Upper*; 100 μm in *A–D*, Lower, *J* and *K*; 50 μm in *I*; and 10 μm in *M*).

blood vessels (Fig. 3*A*) and around endothelial tip cells and their filopodia (Fig. 3*B*). As in the brain, endothelial cells in the retina did not show detectable Nogo-A expression (Fig. 3 *A* and *B*). PDGFRβ$^+$ pericytes partially overlapped with IB4$^+$ endothelial cells but never were present at the tip cell filopodia (Fig. S5 *A–D*). However, endothelial tip cells often colocalized with GFAP$^+$ astrocytic fiber bundles (Fig. S5 *C* and *D*), in agreement with observations described elsewhere (26).

The superficial vascular plexus on the vitreal side of the retina grows from the head of the optic nerve to the retinal periphery during the first postnatal week (Fig. 3*C*) (3, 26). Flat mounts of P4 retinas showed a modest but still significant increase in radial growth of the superficial vascular network in Nogo-A$^{-/-}$ mice compared with their WT littermates (Fig. 3 *E–H*). At P8, when the superficial vascular plexus reached the peripheral margin of the retina, no difference in blood vessel density could be found between Nogo-A$^{-/-}$ and WT mice, on the one hand, and mice treated with anti-Nogo-A antibody and mice treated with control antibody, on the other (Fig. S5 *E–H*). Interestingly, we noticed a dramatic down-regulation in Nogo-A expression in the ganglion cell layer and in the plexiform layer of the retina at P8 (Fig. 3*D*) an age coinciding with the development of the deep retinal vascular layer originating from the endothelial cell sprouting from the superficial retinal plexus (3, 26, 35). At P8, large differences could be observed in the deep retinal vascular layer in Nogo-A$^{-/-}$ mice and animals treated with anti–Nogo-A antibody, on the one hand, and WT mice and mice injected with the control antibody, on the other (Fig. 3 *I–L*). Quantitatively, Nogo-A$^{-/-}$ mice and mice treated with anti–Nogo-A antibody showed increases in blood vessel density in the deep retinal vascular layer of 67 and 44%, respectively, as compared with control animals (Fig. 3*M*). All these data show that Nogo-A negatively regulates the density of forming blood vessels and endothelial tip cells in the brain and in the retina at early postnatal stages.

Nogo-A and Brain Extract Inhibit Adhesion and Spreading of Cultured Brain Vascular Endothelial Cells. Nogo-A exerts its inhibitory effects by two fragments: the Nogo-A– specific fragment Nogo-A Delta 20 (rat amino acids 544–725) and the Nogo-66 sequence (rat amino acids 1019–1083), which is present in Nogo-A, -B, and -C (12, 21). To determine whether Nogo-A can exert direct inhibitory effects on CNS endothelial cells, primary brain-derived MVECs were plated on substrates coated with increasing concentrations of the soluble Nogo-A–specific fragment Delta 20, which is known to exert potent inhibitory effects on growing neurites and spreading fibroblasts (21). Cell spreading and adhesion of MVECs were inhibited by Nogo-A Delta 20 in a dose-dependent manner (Fig. 4 *A–C*). The Nogo-A fragment Delta 21, which has minor inhibitory effects on 3T3 fibroblasts and growing

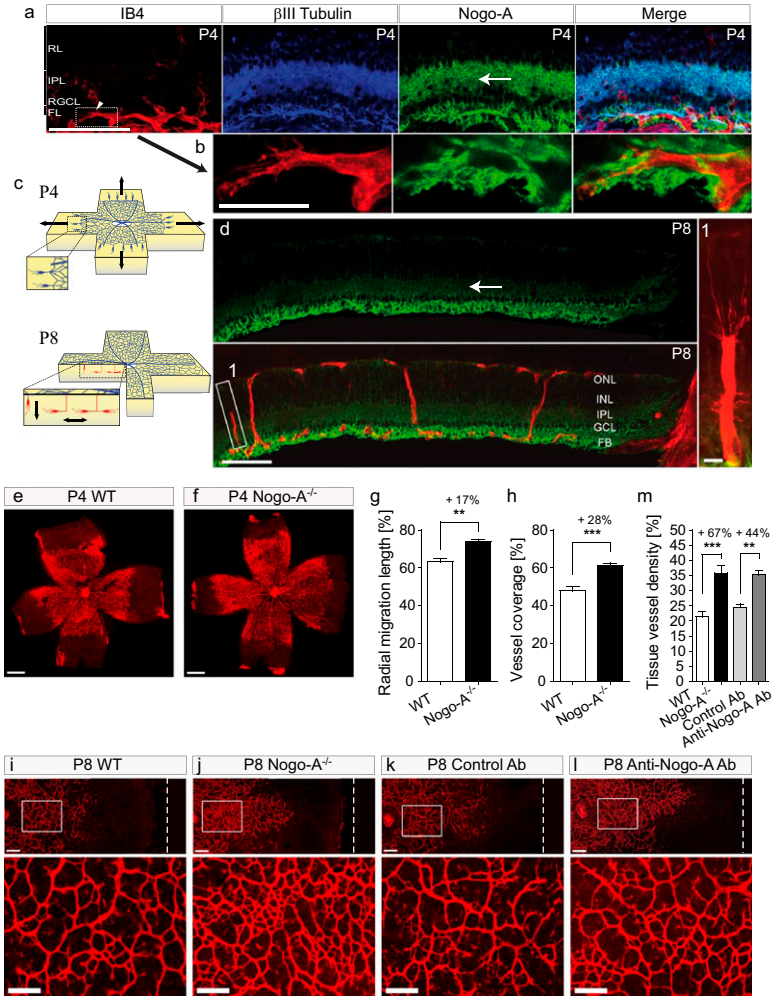

Fig. 3. Nogo-A ablation or neutralization leads to increased tissue density of blood vessels in the postnatal retina. (*A* and *B*) By immunohistochemistry on retinal cryosections, Nogo-A (green) was observed in βIII-tubulin$^+$ neurons (blue) in the close vicinity of IB4$^+$ blood vessels (red) and vascular endothelial tip cells in the mouse retina at P4. (*C*) Schemes showing the development of the superficial (*Upper*, blue) and deep (*Lower*, red) retinal vascular layers at P4 and at P8. Arrows indicate the direction of vascular endothelial (tip) cell migration in the retina. (*D*) The immunofluorescent signal of Nogo-A appeared decreased in the inner plexiform layer of P8 retinal sections (arrow) compared with P4 retinas (*A*) but persisted at a high level in the optic fiber layer. FL, optic fiber layer; IPL, inner plexiform layer; RGCL, retinal ganglion cell layer; RL, retinoblastic layer. (*E* and *F*) The migration front of the superficial vascular layer in IB4-stained P4 retinas was more advanced in Nogo-A$^{-/-}$ animals than in WT control animals. (*G* and *H*) The radial distance of the vascular migration front from the optic nerve head (*G*) and the percentage of retina area covered with vessels (*H*) were significantly increased in P4 retinas of Nogo-A$^{-/-}$ animals as compared with WT controls (mean ± SEM, n = 4–5). (*I*–*K*) Deep retinal vasculature (IB4$^+$) in P8 WT mice (*I*), Nogo-A$^{-/-}$ mice (*J*), and mice treated with control antibody (*K*) or with anti–Nogo-A antibody (*L*). White dashed lines in *I*–*L* *Upper* mark the retinal border. (*M*) Tissue vessel density in the deep vascular layer in retinas of P8 Nogo-A$^{-/-}$ mice and of P8 WT mice injected with anti–Nogo-A antibody was increased significantly as compared with retinas of P8 WT mice or P8 WT mice injected with the isotype control antibody (n = 4–7). All data are shown as mean ± SEM, $^*P < 0.05$, $^{**}P < 0.01$, $^{***}P < 0.001$. (Scale bars: 100 μm in *A*; 25 μm in *B*; 100 μm in *D*; 10 μm in *D*, *Inset*; 500 μm in *E* and *F*; 100 μm in *I*–*L*.)

neurites (21), did not interfere with MVEC adhesion and spreading (Fig. 4 *A*–*C*).

In neurons and in 3T3 fibroblasts, inhibition of neurite growth, adhesion, and spreading by Nogo-A is mediated by the destabilization of the cytoskeleton (12, 36). Phalloidin staining of MVECs placed on Nogo-A Delta 20 for 4 h showed that F-actin had lost its fiber-like organization (Fig. 4*D*), indicating that Nogo-A Delta 20 also acts on the actin cytoskeleton in brain vascular endothelial cells.

To further assess the antiadhesive effect of Nogo-A on brain MVECs, we cultured the cells on a substrate consisting of nanopillar arrays that allowed us to measure the traction/pulling forces exerted by the spreading MVECs on the substrate (Fig. S6 and Movies S1 and S2; the description of nanopillar arrays is given in *SI Materials and Methods*). Nanopillars coated with Nogo-A Delta 20 inhibited MVEC spreading in a dose-dependent manner, in contrast to those coated with Nogo-A Delta 21 (Fig. S6 *A* and *C*). On control nanopillars coated with fibronectin, explorative movements of MVECs exerted an average traction force of 8–10 nN (Fig. S6 *B* and *C*). MVECs plated on Nogo-A Delta 20 at 12.5 pmol/cm^2 or 100 pmol/cm^2 showed decreased pulling forces (~6 nN and ~2 nN, respectively) (Fig. S6 *B* and *C*). On nanopillars coated with Nogo-A Delta 21, the traction forces exerted by the spread MVECs were similar to those on fibronectin (Fig. S6*C*). These results indicate an antiadhesive effect of Nogo-A Delta 20 at the single-cell level.

To mimic the in vivo situation of growing blood vessels invading a Nogo-A–rich CNS tissue, we performed spreading assays of MVECs on dishes coated with either P10 WT or P10 Nogo-A$^{-/-}$ brain membrane protein extract. Adhesion and spreading of MVECs were inhibited by WT extract in a dose-dependent fashion (Fig. S7 *A* and *B*). Extracts from P10 Nogo-A$^{-/-}$ brains had a significantly weaker effect than the extracts from WT brains, suggesting that Nogo-A is an important inhibitor of MVEC spreading in the early postnatal brain (Fig. S7*B*). When dishes coated with WT brain extract were preincubated with the Nogo-A–neutralizing antibody 11C7 before the addition of MVECs, the inhibitory effect of the brain extract was reduced significantly (Fig. S7 *A* and *C*). These results show that endogenous Nogo-A is an important contributor to the inhibitory action of postnatal brain extract on MVEC adhesion and spreading.

Acute Destabilizing Effects of Nogo-A Delta 20 on MVEC Lamellipodia and Filopodia. 1,1′-dioctadecyl-3,3,3′3′-tetramethylindocarbocyanine perchlorate (DiI)-labeled MVECs were cultured for 1 h on a fibronectin-coated nanopillar substrate. They developed a flat, well-spread morphology with typical filopodia and lamellipodia (Fig. 4 *E* and *F*). When Nogo-A Delta 20 was added at a concentration of 1 μM, lamellipodia retracted after 5–10 min (Fig. 4 *G*–*I* and Movies S3 and S4), and the retraction of filopodia began at 40–50 min (Fig. 4 *I* and *J* and Movies S3 and S4). When MVECs were exposed to soluble Nogo-A Delta 21, no retraction of the lamellipodia and filopodia could be observed (Fig. 4 *K*–*N* and Movies S5 and S6). To determine the kinetics of individual filopodium retractions, the bending of nanopillars was monitored after the addition of Nogo-A Delta 20 (Fig. 4*O*). Retraction of a pillar-attached filopodium caused pillar deflection and thereby increased traction forces on the corresponding nanopillars, fol-

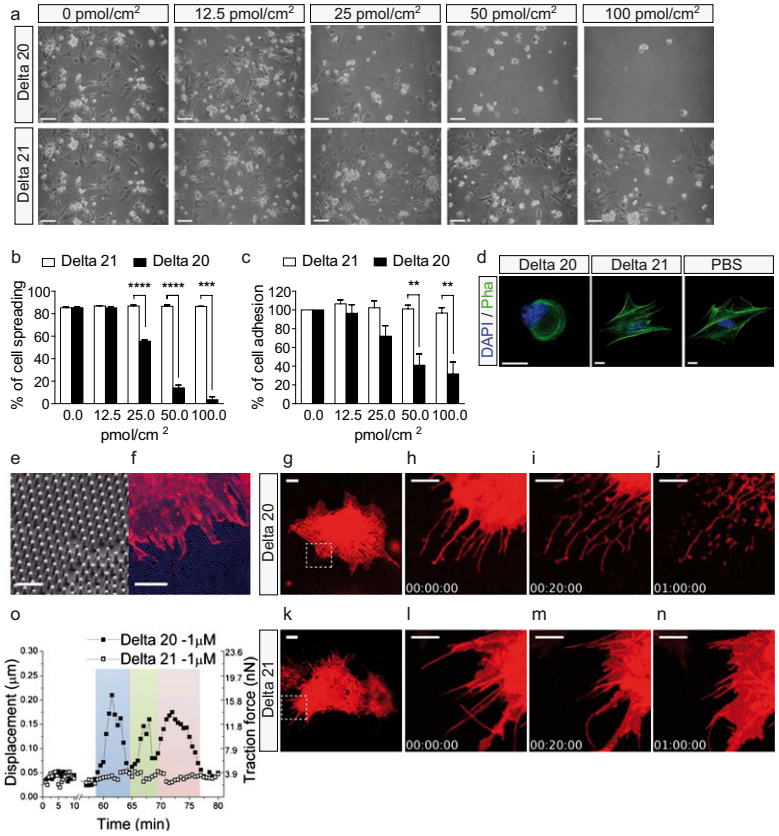

Fig. 4. Nogo-A Delta 20 inhibits the adhesion and spreading of MVECs and exerts a rapid destabilizing effect on MVEC lamellipodia and filopodia. (*A*) MVEC spreading and adhesion were decreased on dishes coated with increasing concentrations of Nogo-A Delta 20. No inhibition of MVEC spreading and adhesion could be seen on dishes coated with Nogo-A Delta 21. (*B* and *C*) MVEC spreading (*B*) and adhesion (*C*) were dose-dependently reduced on dishes coated with Nogo-A Delta 20 but not on dishes coated with Nogo-A Delta 21. (*D*) F-actin (stained with phalloidin) has lost its elongated structure in MVECs grown on dishes coated with Nogo-A Delta 20. DAPI staining is blue. (*E* and *F*) Nanopillar structures (*E*) and a DiI-stained P8 MVEC (red) (*F*) on a nanopillar substrate (blue). (*G*–*N*) Time course of Nogo-A Delta 20-induced retraction of MVEC lamellipodia (*H* and *I*) followed by filopodia retraction (*I* and *J*) over 20 min to 1 h. MVEC treated with Nogo-A Delta 21 showed only minor shape changes (*L*–*N*). Four frames of Movie S3 (*G*–*J*) and of Movie S5 (*K*–*N*) are shown. The boxed areas in *G* and *K* are enlarged successively in *H*–*J* and in *L*–*N*, respectively. (*O*) Retraction of a single MVEC filopodium induced by Nogo-A Delta 20 leads to the bending of a single nanopillar (black squares). The three colors (blue, green, and pink) indicate three complete cycles of attachment, bending, and detachment of the filopodium. MVEC filopodium treated with Nogo-A Delta 21 (white squares) shows only minor net displacements or traction forces of the attached nanopillar. Data shown are mean ± SEM of three replica experiments ($n = 3$). $^{**}P < 0.01$, $^{***}P < 0.001$, $^{****}P < 0.0001$. (Scale bars: 100 µm in *A*; 20 µm in *D*; 2 µm in *E*; 10 µm in *F*, *G*, and *K*; and 5 µm in *H*–*J* and *L*–*N*.)

lowed by detachment and binding to new sites on nanopillars within the reach of the retracting filopodium (Fig. 4*O*). An example with three successive steps of attachment, pulling, and detachment of an individual filopodium is shown in Fig. 4*O*.

No such nanopillar movements were observed upon the addition of Nogo-A Delta 21, and the pulling forces of a filopodium on the nanopillar substrate remained minor, reflecting the normal explorative movements of an MVEC (Fig. 4*O*). These data show that Nogo-A Delta 20 causes an acute and direct destabilization of MVEC lamellipodia and filopodia, structures that are crucial for pathfinding, migration, and sprouting of vascular endothelial cells in vivo.

Nogo-A Delta 20 Inhibits the Migration and Sprouting of Brain Vascular Endothelial Cells In Vitro. To study whether Nogo-A could influence the migration of vascular endothelial cells in the brain, we coated the underside of Transwell inserts with fibronectin mixed with different concentrations of Nogo-A Delta 20 or its inactive neighboring fragment, Nogo-A Delta 21 (Fig. 5*A*). MVECs were plated on the upper side of the inserts, and 10 ng/mL recombinant VEGF-A was added in the bottom well of the chamber to stimulate cell migration (Fig. 5 *A* and *B*) (37). Nogo-A Delta 20 dose-dependently inhibited the fibronectin- and VEGF-stimulated MVEC migration (Fig. 5*C*). The moderate inhibitory effects of Nogo-A Delta 21 on MVEC migration were in agreement with previous observations made in neurons (21).

In the CNS, sprouting angiogenesis is the major process in the development of blood vessels (18). We therefore used an in vitro sprouting angiogenesis assay that reproduces many characteristics of in vivo angiogenesis (38). MVECs coated on beads and cultured in a 3D fibrin matrix grew vessel-like, branched sprouts radially from the beads (Fig. 5*D*). The presence of Nogo-A Delta-20 (1 µM) in the fibrin gel markedly suppressed the formation of these vessel sprouts, the number of branch points, and the length of the sprouts (Fig. 5 *E* and *G*–*I*). Nogo-A Delta-21 did not interfere with endothelial sprout formation (Fig. 5 *F*–*I*).

Nogo-A is an integral membrane protein expressed at the surface of neurons and neuronal-like cells such as PC12 cells or neural stem cells (13, 39–41); therefore, Nogo-A–induced growth inhibition of vascular endothelial cells in the developing brain may be mediated by direct cell–cell contacts. To study this interaction, we plated MVECs onto low-density cultures of PC12 cells, a neuronal cell type expressing high Nogo-A levels at the cell surface (Fig. S8*A*) (41). Within 8–24 h, the MVECs spread and migrated, often forming monolayers in these cultures which contained conspicuous "zones of inhibition" around the PC12 cells (Fig. 5*J*, Fig. S8*B*, and Movie S7). These relatively large zones of inhibition likely resulted from the retraction of migrating MVECs upon contact with PC12 cells (Fig. S8*B* and Movie S7). To analyze the contribution of Nogo-A to this phenomenon of migration restriction, we included blocking antibodies against Nogo-A (11C7). In the presence of these antibodies, the number of zones of inhibition around PC12 cells was greatly reduced (Fig. 5 *K* and *L*). Furthermore, after Nogo-A was silenced by infecting PC12 cells with adenovirus containing the same shRNA used in vivo (Fig. 2 *I*–*L*, ref. 32, and Fig. S8*C*), the number of zones of inhibition was reduced in comparison with the control situation (Fig. 5*L*), to a similar extent as in the antibody-experiments. Whether, in addition to the contact-mediated repulsion, active fragments of Nogo-A were shed by the PC12 cells and thereby formed a repulsive gradient around them could not be determined. Although there is no evidence supporting a possible secretion of Nogo-A to date, this possibility cannot be excluded.

In a different kind of coculture experiment, aggregates of MVECs and PC12 cells were plated at a certain distance, and the interaction of the migrating cell fronts was observed. Without any treatment or in the presence of a control antibody, a clear boundary between the two cell types formed after 48–72 h (Fig. 5 *M* and *N*). However, when Nogo-A was blocked with the neutralizing antibody 11C7, a high degree of mixing of MVECs and PC12 cells was observed at the migrating cell fronts (Fig. 5 *O* and *P*).

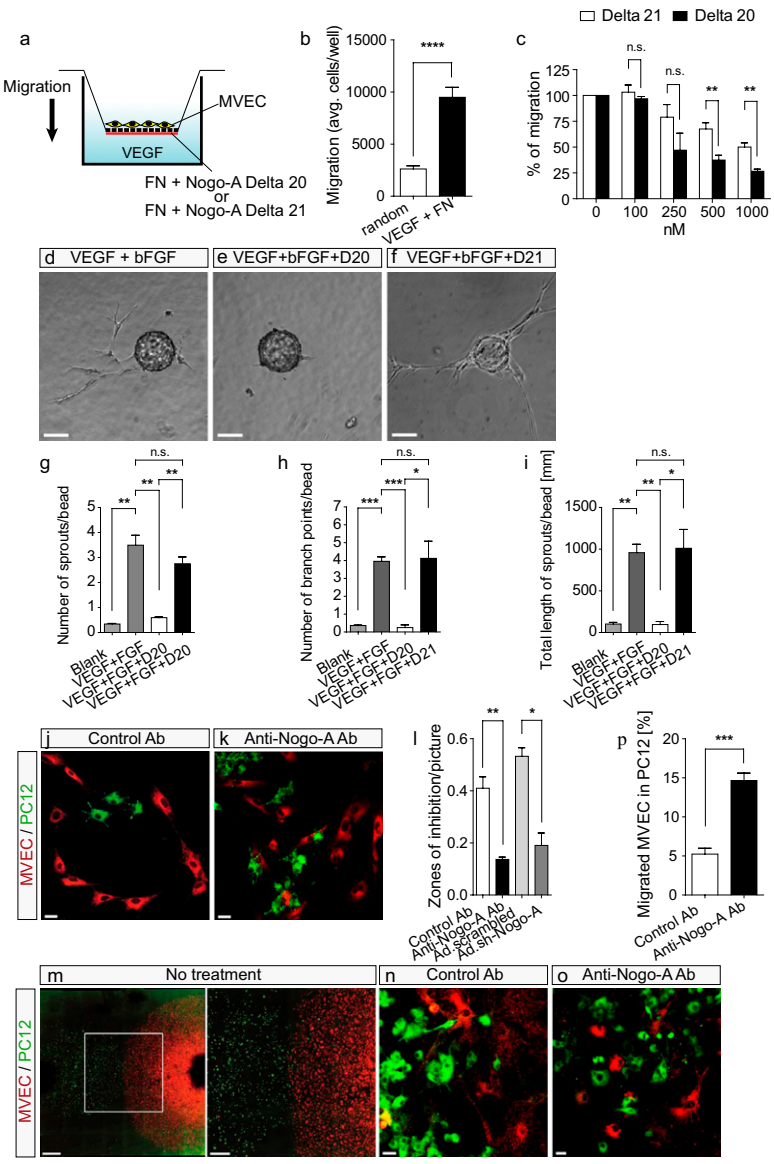

Fig. 5. Nogo-A Delta 20 inhibits microvascular endothelial cell migration and sprouting. (*A*) Scheme of the Transwell system used to investigate MVEC cell migration. (*B*) MVEC migration was increased significantly upon stimulation with a chemotactic (VEGF-A) and a haptotactic (fibronectin, FN) gradient. (*C*) MVEC migration was dose-dependently reduced with increasing concentrations of Nogo-A Delta 20. Note the slight inhibitory activity of Nogo-A Delta 21. Data are shown as mean ± SEM (n = 3–6). (*D–F*) MVEC sprout formation in a 3D fibrin gel containing VEGF-A and basic FGF (bFGF) (*D*) was nearly abolished in the presence of Nogo-A Delta 20 (1 μM) (*E*) but not by Nogo-A Delta 21 (1 μM) (*F*). (*G–I*) MVEC sprout formation was reduced significantly upon the addition of Nogo-A Delta 20. Data are shown as mean ± SEM (n = 3 experiments; at least 25 beads were assayed in each experiment for each condition). (*J* and *K*) In cocultures of brain-derived MVECs with neuronal PC12 cells expressing Nogo-A, PKH26-labeled MVECs (red) formed zones of inhibition around PKH67-stained PC12 cells (green) (*J*). Zones of inhibition were reduced and both cell types intermixed in the presence of the neutralizing anti–Nogo-A antibody (*K*). (*I*) Significantly fewer zones of inhibition were formed by MVECs around PC12 cells in the presence of the anti–Nogo-A antibody (11C7) or when Nogo-A was down-regulated using Ad.sh-RNA-Nogo-A virus. Data are shown as mean ± SEM (n = 3). (*M*) Encounter of migration fronts of PKH26-stained MVECs (red) and PKH67-stained PC12 cells (green) migrating from plated droplets. The boxed area is enlarged at right. Note the formation of a clearly separated interface. (*N* and *O*) The presence of anti–Nogo-A antibody reduced significantly the Nogo-A–mediated segregation of MVECs and PC12 cells, as shown quantitatively in *P* by the mixture of MVECs and PC12 cells. Data are shown as mean ± SEM (n = 4–5 experiments; two or three cultures were evaluated per condition and experiment). $*P < 0.05$, $**P < 0.01$, $***P < 0.001$, $****P < 0.0001$. (Scale bars: 100 μm in *D–F*; 20 μm in *J* and *K*; 1,000 μm in M, *Left*; 200 μm in *M*, *Right*; and 20 μm in *N* and *O*.)

Taken together, these results suggest that the presence of Nogo-A on the surface of neuronal cells exerts a repulsive action on migrating vascular endothelial cells in the brain.

Nogo-66 Does Not Affect Brain Endothelial Cell Adhesion, Migration, or Filopodia and Lamellipodia Motility. To test whether the Nogo-66 sequence of Nogo-A, which activates the receptor complex composed of glycosylphosphatidylinositol (GPI)-linked leucine rich repeat (LRR) protein Nogo receptor 1 (NgR1) and leucine rich repeat and Ig domain containing 1 (Lingo1), may affect brain vascular endothelial cells, we first investigated the expression pattern of the Nogo-66 receptor components NgR1 (12) and Lingo1 (12) in the CNS vasculature. Neither NgR1 nor Lingo1 were detectable at the protein level in isolated CNS endothelial cells (MVECs), but they were present in brain extracts as revealed by Western blot analysis (Fig. 6*A*). Immunofluorescent staining confirmed the expression of NgR1 in the brain parenchyma of P8 cortical sections (Fig. 6*B*), in accordance with earlier reports (42). However, NgR1 was not detectable on endothelial cells and their filopodial protrusions in the CNS (Fig. 6*B*).

Next, to determine whether functional Nogo-66 exerts inhibitory effects on MVECs and their motility, we plated MVECs on nanopillars coated with increasing concentrations of Nogo-66. The spreading of MVECs was not affected even at very high concentrations of Nogo-66, in contrast to MVECs plated on nanopillars coated with Nogo-A Delta 20 (Fig. S9 *A* and *B*). At the single-cell level, MVECs on Nogo-66 did not show inhibition of either cell adhesion or of the generation of traction force (Fig. 6 *C* and *D* and Fig. S9*C*). In contrast to our observations on Nogo-A Delta 20–coated surfaces, MVECs displayed well-spread morphologies with extension of numerous lamellipodial and filopodial protrusions, similar to MVECs plated on fibronectin-coated nanopillars (Fig. 6*C* and Movie S8). In addition to its inhibitory effects on neurite outgrowth, Nogo-66 has been shown to induce collapse of growth cones in dorsal root ganglion neurons (21). Addition of soluble Nogo-66 (1 μM) did not cause lamellipodial or filopodial retraction in MVECs on fibronectin-coated nanopillars (Fig. 6 *E–G* and Movie S9), and in these conditions the changes in the pulling forces exerted by a single MVEC filopodium on nanopillar structures were modest (Fig. 6*H*). Finally, when coated on the underside of Transwell inserts, a wide range of Nogo-66 concentrations did not inhibit MVEC migration, in contrast to Nogo-A Delta 20 (Fig. 6*I*).

Taken together, these results show that the Nogo-66–NgR1 complex has no inhibitory effect on CNS endothelial cell adhesion or migration or on lamellipodia and filopodia dynamics in vitro.

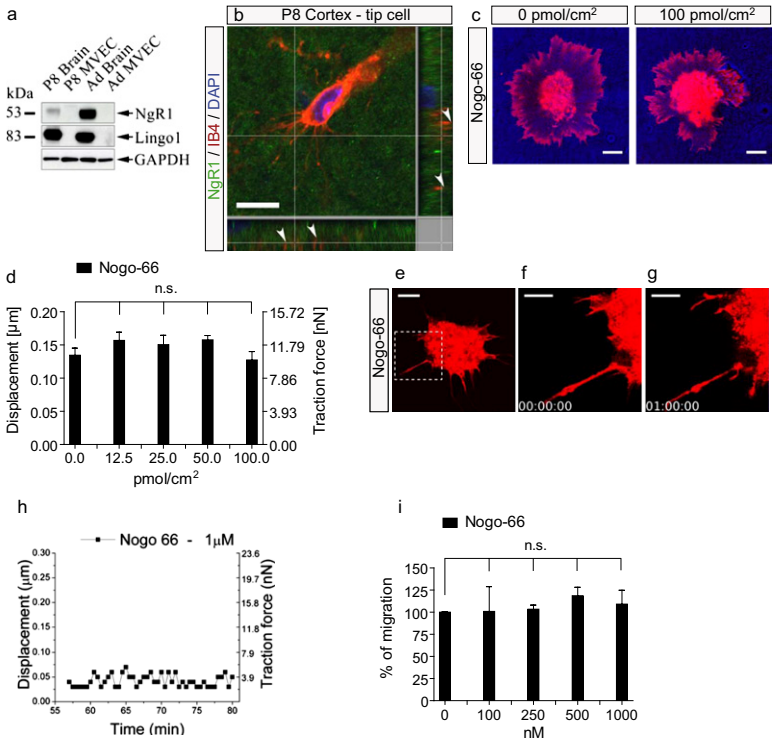

Fig. 6. Nogo-66 does not inhibit microvascular endothelial cell adhesion, migration, or actin cytoskeleton dynamics. (*A*) Western blot using a rabbit anti-NgR1 and a rabbit anti-Lingo1 antibody. NgR1 and Lingo1 were detected in P8- and adult brain membrane extracts but not in P8- and adult brain-derived MVECs. GAPDH was used as loading control (25 µg protein per lane). (*B*) NgR1 (green) is expressed in the vicinity of an IB4-labeled endothelial tip cell and its filopodial protrusions (red) in a P8 cortex. Note the punctate NgR1 labeling. Arrowheads indicate IB4$^+$ but NgR1-negative endothelial tip cell filopodia. (*C*) DiI-labeled MVECs were added onto a nanopillar substrate. MVEC spreading was not decreased on a substrate consisting of nanopillars coated with increasing concentrations of Nogo-66. (*D*) Displacement and traction force generated by MVECs on nanopillars coated with Nogo-66 were not decreased and were comparable to those on fibronectin-coated nanopillars. Nanopillars in contact with three individual MVECs were measured for every condition, over a time period of 10 min. Data are shown as mean ± SEM of three single MVECs per group (n = 3). (*E*–*G*) Three frames of Movie S9 are shown. Nogo-66 (1 µM) did not cause retraction of MVEC lamellipodia and filopodia over a 1-h period. Minor changes in MVEC shape reflect explorative behaviors of MVEC protrusions. The boxed area in *E* is enlarged in *F* and *G*. (*H*) For MVECs treated with Nogo-66 (1 µM), single MVEC filopodia exerted only small net displacements and traction forces on the attached nanopillars. (*I*) No inhibition of MVEC migration was observed with increasing concentrations of Nogo-66. Data are shown as mean ± SEM of three replica experiments (n = 3). (Scale bars: 10 µm in *B*, *C*, and *E*; 5 µm in *F* and *G*.)

Nogo-A Delta 20–Induced Inhibitory Effects on Brain Endothelial Cells Depend on the Rho-A–ROCK–Myosin II Pathway. In neurons, Nogo-A Delta 20 and Nogo-66 lead to the intracellular activation of the Ras homolog gene family, member A (Rho-A)-Rho-associated, coiled-coil containing protein kinase (ROCK) pathway and to subsequent inhibition of neurite outgrowth (12, 36, 43). To address the molecular mechanisms responsible for the inhibitory effects of Nogo-A Delta 20 on brain vascular endothelial cells, we used pharmacological inhibitors of different proteins participating in Nogo-A Delta 20 signaling in neurons and 3T3 fibroblasts (44). The inhibition of Rho and ROCK by C3-transferase (44) or Y27632 (44), respectively, prevented the inhibitory effects of Nogo-A Delta 20 on MVEC cell spreading (Fig. 7 *A*–*C*, Fig. S10 *A*–*C*, and Movies S10, S11, and S12) and the generation of traction force on the Nogo-A Delta 20–coated nanopillar substrate (resulting in traction forces of ∼10 nN) (Fig. 7*F*). Both blockers led to an endothelial cell morphology characterized by increased cell spreading and more abundant lamellipodial and filopodial protrusions on the Nogo-A Delta 20–coated nanopillars than in the nontreated controls (Fig. 7 *A*–*C*, Fig. S10 *A*–*C*, and Movies S10, S11, and S12). Consistent with these findings, on flat surfaces, the addition of Y27632 almost completely prevented the inhibitory action of Nogo-A Delta 20 on MVEC spreading (Fig. S11).

To determine whether Myosin II is involved in Nogo-A Delta 20–induced retraction of the actin cytoskeleton, we pharmacologically blocked the myosin light-chain kinase (MLCK) with ML-7 (45) as well as the Myosin II ATPase with Blebbistatin (46). Both blockers prevented the inhibitory effect of Nogo-A Delta 20 on MVEC cell adhesion (Fig. 7 *A*, *D*, and *E* and Movies S10, S13, and S14) and on the generation of traction forces (Fig. 7*F*).

To study potential effects on single filopodia, we preincubated MVECs in suspension with these inhibitors. When plated on fibronectin-coated nanopillar substrates, the subsequent addition of Nogo-A Delta 20 in soluble form (1 µM) did not cause lamellipodial or filopodial retraction in these MVECs treated with C3 transferase (Fig. S12 *A*–*D* and Movie S15), Y27632 (Fig. S12 *E*–*H* and Movie S16), ML-7 (Fig. S12 *I*–*L* and Movie S17), or Blebbistatin (Fig. S12 *M*–*P* and Movie S18). At the level of single endothelial protrusions, nanopillar-attached MVEC filopodia showed normal, explorative movements and exerted small traction/pulling forces on the substrate, similar to observations in MVECs treated with Nogo-A Delta 21 (Fig. 7 *G* and *H*).

Taken together, these results demonstrate a central role for the Rho–ROCK–Myosin II axis in the signal transduction of Nogo-A Delta 20–mediated inhibition of brain vascular endothelial cells. The VEGF-A–VEGFR2–VEGFR2-Delta-like ligand 4 (Dll4)–Notch pathway is known to be an important regulator of CNS angiogenesis (18) and endothelial tip cell formation (37, 47-49). To investigate whether the VEGF-A–VEGFR2–Dll4–Notch signaling pathway was affected by Nogo-A gene deletion, we compared the expression levels of these proteins in P8 WT and P8 Nogo-A$^{-/-}$ brains. Protein levels of phosphorylated—and thus activated—VEGFR2 and of total VEGFR2 were unchanged in the P8 WT and P8 Nogo-A$^{-/-}$whole-brain lysates (Fig. S13*A*). In addition, no significant changes could be observed in the mRNA levels of VEGF-A, VEGFR2, Dll4, and Notch4 (Fig. S13*C*). Furthermore, in MVECs treated with Nogo-A Delta 20, the levels of p-VEGFR2 and total VEGFR2 were not decreased (Fig. S13*B*). These results suggest that Nogo-A's negative regulatory effect on CNS angiogenesis in vivo and on MVEC motility in vitro occurs independently of the VEGF-A–VEGFR2–Dll4–Notch signaling axis.

Discussion

Using in vitro and in vivo approaches, we showed that the neurite growth-inhibitory membrane protein Nogo-A is a negative regulator of angiogenesis in the postnatal CNS. Our results suggest that the Nogo-A–specific domain Nogo-A Delta 20 inhibits spreading, adhesion, and migration of MVECs via the Rho-A–ROCK–Myosin II pathway. We propose that, by acting on the cytoskeleton of CNS endothelial tip cells and their filopodia, Nogo-A controls the sprouting and migration of growing CNS blood vessels.

After the initial development of the meningeal vascular plexus, the CNS is vascularized almost exclusively by sprouting angiogenesis, defined as the growth of new blood vessels from preexisting ones (18, 50). In this process, endothelial tip cells elaborate filopodial extensions that sense guidance molecules in their environment to steer the migrating blood vessel in the CNS paren-

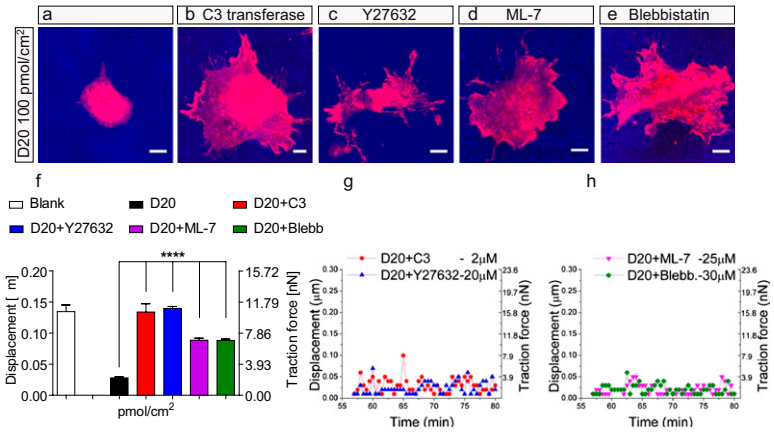

Fig. 7. The inhibitory effect of Nogo-A Delta 20 on the spreading of brain MVECs can be counterbalanced by blocking the Rho-A-ROCK-Myosin II pathway. (*A*) MVEC spreading was decreased on a substrate consisting of nanopillars coated with Nogo-A Delta 20 (100 pmol/cm^2). (*B*–*E*) Treatment with blockers of Rho with 2 μM C3 transferase (*B*), ROCK with 20 μM Y27632 (*C*), MLCK with 25 μM ML-7 (*D*), and Myosin II ATPase with 30 μM Blebbistatin (*E*) counterbalanced the inhibitory action of Nogo-A Delta 20 on MVEC spreading. (*F*) Displacement and traction force generated by MVECs treated with the blockers C3 transferase, Y27632, ML-7, and Blebbistatin on nanopillars coated with Nogo-A Delta 20 were increased to levels similar to those generated by untreated MVECs on nanopillars coated with Nogo-A Delta 21 (see *Fig. S6*). Nanopillars in contact with three individual MVECs were measured for every condition, over a time period of 10 min. ****$P <$ 0.0001. Data are shown as mean ± SEM of three single MVECs per group (n = 3). (*G* and *H*) For MVECs treated either with C3 transferase or Y27632 (*G*), or with ML-7 or Blebbistatin (*H*) single MVEC filopodia exerted only small net displacements and traction forces on the attached nanopillars. Data are shown as mean ± SEM of three replica experiments (n = 3). (Scale bars: 10 μm.)

chyma. In contrast to the predominant role of VEGF as a positive regulator of angiogenesis (18, 51), negative regulators such as semaphorins, netrins, and slits recently have been recognized (2), especially in the retina; however, much less is known about how the vascularization in the brain is regulated. Here we found that Nogo-A is an important negative regulator of the formation of the postnatal CNS vascular network, in various brain regions as well as in the retina. Our in vitro results from a variety of assays suggest that, by exerting inhibitory effects on the adhesion and the migration of vascular endothelial cells, Nogo-A could control the sprouting of blood vessels into the postnatal CNS parenchyma and thereby slow blood vessel formation. The attenuation of blood vessel formation by Nogo-A is strongly suggested by the hypervascularization observed in P4 and P8 Nogo-A knockout mice and in mice treated postnatally with a function-blocking anti–Nogo-A antibody in vivo. Other factors and membrane proteins such as VEGF-A and FGF-2, as well as semaphorins, slits, netrins, and ephrins (2, 52, 53), act simultaneously as axonal guidance molecules and as factors regulating the growth of blood vessels. Our results suggest that, in addition to its role in axonal growth (9, 12), neuronal Nogo-A also regulates vascular endothelial tip cells and thereby influences vessel density in the developing CNS.

At the adult stage, a main function of Nogo-A is believed to be the stabilization of the CNS wiring and the restriction of growth and plasticity (12). These effects are mediated via repulsive and growth-inhibitory effects on the cytoskeleton of the growth cone as well as through transcription-dependent mechanisms in the neuronal cell body (12). During development, neuronal or glial Nogo-A can inhibit the migration, adhesion, and branching of neurons (9, 10, 12). Comparable to the process of axonal guidance and neurite growth, endothelial tip cells are guided via a balanced interplay of growth-promoting and growth-restricting factors (1). Here we show that Nogo-A Delta 20 blocked CNS endothelial cell migration and spreading in a Rho-A–ROCK–Myosin–dependent manner. Rho-GTPases, ROCK, and Myosin II have been shown to regulate negatively lamellipodia and filopodia formation in endothelial cells (54–56). In this study, we observed that the inhibition of Rho-A and ROCK prevented filopodial retraction induced by Nogo-A Delta 20, suggesting that common mechanisms mediate the Nogo-A–induced cytoskeleton destabilization in endothelial and neuronal cells (12, 36, 57).

Nogo-A knockout in vivo or Nogo-A addition to MVECs did not change the expression of VEGF-A, VEGFR2, Dll4, or Notch or the activation level of VEGFR2. This result is interesting in light of this signaling system's important role in CNS angiogenesis (18) and endothelial tip cell formation (37, 47–49). Whether and where the VEGF- and the Nogo-A–signaling pathways intersect intracellularly deserves further investigation.

In the mature CNS, vascular endothelial cells are not in direct contact with neurons. Therefore, it is tempting to speculate that the repulsive effects mediated by neuronal Nogo-A on endothelial cells could contribute to the segregation of these two cell types.

Our results with the active Nogo-A fragment Delta 20 indicate that the effects of Nogo-A on developmental CNS angiogenesis are mediated via the Nogo-A–specific region of the protein. This notion is supported by our findings that the second inhibitory domain of Nogo-A, Nogo-66, which is present in Nogo-A, -B, and -C, did not exert inhibitory effects on MVEC cell adhesion or migration or on MVEC filopodia and lamellipodia motility. In addition, protein members of the Nogo-66 receptor complex, NgR1 and Lingo1, were not expressed on CNS endothelial tip cell filopodia or in isolated MVECs. Therefore, although in neurons Nogo-A exerts inhibitory effects on neurite outgrowth via Nogo-A Delta 20 and Nogo-66 (12, 21), only Nogo-A Delta 20 is inhibitory for the motility of brain endothelial cells. The seemingly contradictory recent finding that NgR1 antibody-loaded hydrogels implanted into a spinal cord lesion enhanced axonal growth as well as angiogenesis may result from the cellular complexity of the inflammatory, scarring, and regenerative reactions in this experimental paradigm (58). Furthermore, it remains to be determined whether members of the Nogo-66 receptor complex such as NgR1, Lingo1, and also p75, TROY, and PirB (12), may be expressed on angiogenic endothelial cells in pathological conditions. The present results in the CNS also differ significantly from the effects of Nogo-B in the peripheral vasculature. Nogo-B has promigratory and proadhesive effects on non-CNS vascular endothelial cells in vitro (14, 15), and its loss after vessel damage leads to pathological thickening of peripheral blood vessels in the mouse in vivo (14, 16). These effects are mediated by a Nogo-B–specific receptor, NgBR, which does not interact with Nogo-A (15, 17). Nogo-B receptor activation also is proangiogenic in the zebrafish embryo (17). Nogo-A's antiangiogenic and Nogo-B's proangiogenic effects also might counteract each other, as suggested by the recent finding showing that ear skin angiogenesis was not affected in Nogo-A/B double-knockout mice (59). Furthermore, although Nogo-A destabilizes the actin cytoskeleton by activating the Rho-A–ROCK–Myosin II pathway in endothelial cells, the activation of Ras-related C3 botulinum toxin substrate 1 (Rac1) by Nogo-B results in proadhesive and promigratory responses, at least in macrophages (59). The opposite effects exerted by Nogo-A and -B are intriguing, but whether Nogo-A and -B also could antagonize each other's angiogenic effects in the CNS remains to be determined.

In addition to its expression in the CNS, Nogo-A also is expressed in non-CNS tissues such as the embryonic skin (predominantly around hair bulges), embryonic teeth, and in the developing and adult heart (12, 13). However, it is not known to date whether Nogo-A also can affect vascular beds outside the CNS. Given the important negative regulatory effects of Nogo-A on CNS

angiogenesis and the proangiogenic effects of Nogo-B on peripheral blood vessels and endothelial cells (14, 15, 17), future studies should investigate the possible functions of Nogo-A on angiogenesis and vascular beds outside the CNS.

During developmental angiogenesis, the neurovascular interactions are controlled by the expression of guidance molecules in neurons such as netrins, semaphorins, ephrins, slits, and wingless-type proteins (wnts) that activate specific receptors on endothelial cells (23). Because we examined blood vessel density in early postnatal brains at a time when myelination was only starting (P0–P8) and Nogo-A is expressed mostly by neurons (12), migrating vascular endothelial cells interacted mainly with neuronal Nogo-A during this period. Furthermore, our results suggest that perivascular cells such as pericytes and astrocytes do not prevent contacts between neuronal processes and tip cell filopodia. Because Nogo-A Delta 20 cannot bind to the known Nogo receptors NgBR and NgR1 (12), we propose that neuronal Nogo-A Delta 20 activates a Nogo-A–specific but as yet unidentified receptor on CNS endothelial cells.

Neurovascular interactions also may explain why Nogo-A deletion led to less pronounced effects in the superficial retinal vascular plexus than in the deeper retinal vascular plexus. Whereas endothelial cells mainly contact astrocytes in the superficial plexus as they migrate radially at the surface of the retinal tissue, they cross Nogo-A–expressing neuronal layers during their migration into the inner retina to form the deeper retinal vascular plexus (26).

Interestingly, amino Nogo-A also has been reported to disturb the interactions between integrins and the extracellular matrix (ECM), a process through which Nogo-A could inhibit the formation of focal adhesions between the cell membrane and its substrate (60). In our study, the fact that MVECs could not deflect Nogo-A Delta 20–coated nanopillars may reflect similar integrin–fibronectin contact disturbances. Indeed, we also observed that substrate-bound Nogo-A Delta 20 strongly inhibited MVEC spreading and migration that requires traction forces relying onto integrin-ECM anchorages (61). Therefore, it is possible that the antiadhesive effects of Nogo-A Delta 20 on endothelial cells are mediated by the cytoskeleton disassembly and by the disturbance of adhesive interactions between the cell membrane and the ECM.

In addition to neuronal Nogo-A, Nogo-A expression by oligodendrocytes also may affect CNS angiogenesis, because CNS white matter is well known to be much less densely vascularized than CNS gray matter (19). Thus, myelin-derived Nogo-A may be one factor restricting blood vessel growth in CNS white matter in development and later in adulthood.

The observed effects of Nogo-A inactivation on postnatal CNS angiogenesis were compensated at the adult stage. The transitory nature of the hypervascularization might be explained by compensatory mechanisms involving other angiogenic molecules. Similarly, both Netrin1 and Roundabout4 (Robo4) can inhibit angiogenesis by interacting with Unc-5 homolog B (UNC5B) expressed on endothelial cells (62, 63). Although UNC5B deletion results in hypervascularization, the ablation of Netrin1 or Robo4 does not cause obvious vascular phenotypes in adult mice. Importantly, blood vessel density is influenced strongly by the metabolic demand of the tissue. In the retina, ganglion cells control the production of the proangiogenic factors VEGF and angiopoietin1/2 and thereby regulate blood vessel growth (64). The vascular phenotype observed after Nogo-A ablation thus may be corrected during postnatal life by the adjustment of other angiogenic factors depending on the neuronal metabolic requirements. Because there also is a tight link between neuronal activity, regional cerebral blood flow, and blood vessel density (65), these activity-dependent mechanisms may compensate and override Nogo-A's influence on postnatal CNS angiogenesis.

Angiogenesis plays crucial roles in the pathophysiology of various CNS diseases. Therefore one may speculate that Nogo-A also could influence vessel repair and sprouting, for example after ischemic stroke or spinal cord injury, in retinopathies, or in brain tumors. Acute and delayed treatment with anti–Nogo-A antibody was shown to enhance compensatory neurite sprouting, regeneration, rewiring, and functional recovery (66, 67). Nogo-A is up-regulated around the lesion site in a stroke model (68), but the vascular rearrangements and a potential proangiogenic effect in the peri-infarct zone (e.g., of an acute Nogo-A–suppressive treatment) have not been studied yet. Axon guidance molecules also are involved in ischemic conditions in the retina. For example, the axon guidance molecules Semaphorin 3A (69) and Semaphorin 3E (70) are secreted by neurons in the hypoxic retina and act as vasorepulsive factors (69). The secretion of semaphorins by ischemic neurons prevented newly formed vessels from entering the avascular retina and instead misguided them toward the vitreous body, causing its aberrant hypervascularization. Silencing Semaphorin 3A enhanced normal vascular regeneration, diminished aberrant neovascularization, and thereby preserved neuroretinal function (69). In a model of ocular hypertension in which the blood supply also is altered, Nogo-A was up-regulated in retinal ganglion cells (71). Therefore, similarly to semaphorins, the increase of Nogo-A at the surface of ischemic neurons may restrict neovascularization in pathological conditions.

With regard to brain tumors, Nogo-A has been proposed as a marker allowing differentiation among the various types of human gliomas, with a higher Nogo-A expression in oligodendrogliomas than in the more densely vascularized glioblastomas (72). Furthermore, it was reported previously that Nogo-A expression correlated negatively with the malignancy grade of oligodendrogliomas (73). In this case, a high expression of Nogo-A may restrict vascularization of the oligodendroglioma and thereby limit the tumor growth. Another study reported that the splicing factor polypyrimidine tract-binding protein 1 (PTBP1) repressed Nogo-A protein translation and increased the proliferation of human glioma cell lines (74), but ectopic Nogo-A overexpression slowed the glioma cell proliferation (74). These data therefore suggest that, in addition to exerting a cell-autonomous effect on tumor cell division, PTBP1 may control the glioblastoma vascularization process by regulating the expression of Nogo-A in glioma cells.

In conclusion, the present results demonstrate a role for Nogo-A as an important negative regulator of angiogenesis in the developing CNS.

Materials and Methods

To investigate Nogo-A's influence on CNS angiogenesis, we used a combination of various in vivo and in vitro methods.

The in vivo methods used were genetically modified mice (Nogo-A KO mice), i.p. injections of anti–Nogo-A antibody, intracerebroventricular injections of adeno-associated virus (down-regulation of Nogo-A), immunofluorescent staining of brain and retina sections, analysis of brain and retinal vessel density, analysis of cortical endothelial tip cells, and analysis of perfused brain vessels using Evans blue.

In vitro methods consisted in the isolation of primary brain-derived MVECs, MVEC and PC12 cell culture, preparation of P10 brain extracts, adhesion assays, spreading assays, transmigration assays, sprouting angiogenesis assays, encounter assays, droplet encounter assays, adenovirus-mediated down-regulation of Nogo-A in PC12 cells, nanopillars arrays, traction force measurements, time-lapse video microscopy, single filopodia analysis, Western blot analysis, and quantitative real-time PCR.

For a detailed description of these topics, please see *SI Materials and Methods*.

ACKNOWLEDGMENTS. We thank our colleagues Dana Dodd, Franziska Christ, Barbara Weber, Regula Schneider, Caroline Aemisegger, Jose Maria Matéos, Sandrine Joly, and Olivier Raineteau for help with cell culture and imaging; Annika Armulik for providing the anti-PDGFRβ antibody; and Novartis for providing the anti–Nogo-A antibody 11C7. This work was supported by grants from the National Centre for Competence in Research "Neural Plasticity and Repair" of the Swiss National Science Foundation and the European Union's Seventh Framework Programme (FP7/2008-2013) under Grant Agreement 201024 Affording Recovery in Stroke; the Livesense Project funded by the Swiss National Science Foundation (Nano-Ttera.ch); and a European Research Council Advanced Grant (to V.V.). T.W. was supported by an MD-PhD fellowship from the Swiss National Science Foundation and by the Olga Mayenfisch Foundation, the Hartmann Muller Foundation, the Theodor and Ida Herzog Egli Foundation, and the EMDO Foundation.

1. Carmeliet P, Tessier-Lavigne M (2005) Common mechanisms of nerve and blood vessel wiring. *Nature* 436(7048):193–200.
2. Adams RH, Eichmann A (2010) Axon guidance molecules in vascular patterning. *Cold Spring Harb Perspect Biol* 2(5):a001875.
3. Gerhardt H, et al. (2003) VEGF guides angiogenic sprouting utilizing endothelial tip cell filopodia. *J Cell Biol* 161(6):1163–1177.
4. De Smet F, Segura I, De Bock K, Hohensinner PJ, Carmeliet P (2009) Mechanisms of vessel branching: Filopodia on endothelial tip cells lead the way. *Arterioscler Thromb Vasc Biol* 29(5):639–649.
5. Segura I, De Smet F, Hohensinner PJ, Ruiz de Almodovar C, Carmeliet P (2009) The neurovascular link in health and disease: An update. *Trends Mol Med* 15(10):439–451.
6. Chen MS, et al. (2000) Nogo-A is a myelin-associated neurite outgrowth inhibitor and an antigen for monoclonal antibody IN-1. *Nature* 403(6768):434–439.
7. Schwab ME (2004) Nogo and axon regeneration. *Curr Opin Neurobiol* 14(1):118–124.
8. GrandPré T, Nakamura F, Vartanian T, Strittmatter SM (2000) Identification of the Nogo inhibitor of axon regeneration as a Reticulon protein. *Nature* 403(6768): 439–444.
9. Petrinovic MM, et al. (2010) Neuronal Nogo-A regulates neurite fasciculation, branching and extension in the developing nervous system. *Development* 137(15): 2539–2550.
10. Mathis C, Schröter A, Thallmair M, Schwab ME (2010) Nogo-a regulates neural precursor migration in the embryonic mouse cortex. *Cereb Cortex* 20(10):2380–2390.
11. Mingorance A, et al. (2004) Regulation of Nogo and Nogo receptor during the development of the entorhino-hippocampal pathway and after adult hippocampal lesions. *Mol Cell Neurosci* 26(1):34–49.
12. Schwab ME (2010) Functions of Nogo proteins and their receptors in the nervous system. *Nat Rev Neurosci* 11(12):799–811.
13. Huber AB, Weinmann O, Brösamle C, Oertle T, Schwab ME (2002) Patterns of Nogo mRNA and protein expression in the developing and adult rat and after CNS lesions. *J Neurosci* 22(9):3553–3567.
14. Acevedo L, et al. (2004) A new role for Nogo as a regulator of vascular remodeling. *Nat Med* 10(4):382–388.
15. Miao RQ, et al. (2006) Identification of a receptor necessary for Nogo-B stimulated chemotaxis and morphogenesis of endothelial cells. *Proc Natl Acad Sci USA* 103(29): 10997–11002.
16. Kritz AB, et al. (2008) In vivo modulation of Nogo-B attenuates neointima formation. *Mol Ther* 16(11):1798–1804.
17. Zhao B, et al. (2010) Nogo-B receptor is essential for angiogenesis in zebrafish via Akt pathway. *Blood* 116(24):5423–5433.
18. Mancuso MR, Kuhnert F, Kuo CJ (2008) Developmental angiogenesis of the central nervous system. *Lymphat Res Biol* 6(3-4):173–180.
19. Zeller K, Vogel J, Kuschinsky W (1996) Postnatal distribution of Glut1 glucose transporter and relative capillary density in blood-brain barrier structures and circumventricular organs during development. *Brain Res Dev Brain Res* 91(2):200–208.
20. Foran DR, Peterson AC (1992) Myelin acquisition in the central nervous system of the mouse revealed by an MBP-Lac Z transgene. *J Neurosci* 12(12):4890–4897.
21. Oertle T, et al. (2003) Nogo-A inhibits neurite outgrowth and cell spreading with three discrete regions. *J Neurosci* 23(13):5393–5406.
22. Daneman R, Zhou L, Kebede AA, Barres BA (2010) Pericytes are required for blood-brain barrier integrity during embryogenesis. *Nature* 468(7323):562–566.
23. Quaegebeur A, Lange C, Carmeliet P (2011) The neurovascular link in health and disease: Molecular mechanisms and therapeutic implications. *Neuron* 71(3):406–424.
24. Armulik A, et al. (2010) Pericytes regulate the blood-brain barrier. *Nature* 468(7323): 557–561.
25. Dorrell MI, Aguilar E, Friedlander M (2002) Retinal vascular development is mediated by endothelial filopodia, a preexisting astrocytic template and specific R-cadherin adhesion. *Invest Ophthalmol Vis Sci* 43(11):3500–3510.
26. Fruttiger M (2007) Development of the retinal vasculature. *Angiogenesis* 10(2):77–88.
27. Simonen M, et al. (2003) Systemic deletion of the myelin-associated outgrowth inhibitor Nogo-A improves regenerative and plastic responses after spinal cord injury. *Neuron* 38(2):201–211.
28. Dimou L, et al. (2006) Nogo-A-deficient mice reveal strain-dependent differences in axonal regeneration. *J Neurosci* 26(21):5591–5603.
29. Liebscher T, et al. (2005) Nogo-A antibody improves regeneration and locomotion of spinal cord-injured rats. *Ann Neurol* 58(5):706–719.
30. Engelhardt B (2003) Development of the blood-brain barrier. *Cell Tissue Res* 314(1): 119–129.
31. Göbel U, Theilen H, Kuschinsky W (1990) Congruence of total and perfused capillary network in rat brains. *Circ Res* 66(2):271–281.
32. Pernet V, et al. (2012) Neuronal Nogo-A upregulation does not contribute to ER stress-associated apoptosis but participates in the regenerative response in the axotomized adult retina. *Cell Death Differ* 19(7):1096–1108.
33. Pradhan AD, et al. (2010) Dendritic spine alterations in neocortical pyramidal neurons following postnatal neuronal Nogo-A knockdown. *Dev Neurosci* 32(4):313–320.
34. Stahl A, et al. (2010) The mouse retina as an angiogenesis model. *Invest Ophthalmol Vis Sci* 51(6):2813–2826.
35. Stefater JA, 3rd, et al. (2011) Regulation of angiogenesis by a non-canonical Wnt-Flt1 pathway in myeloid cells. *Nature* 474(7352):511–515.
36. Nash M, Pribiag H, Fournier AE, Jacobson C (2009) Central nervous system regeneration inhibitors and their intracellular substrates. *Mol Neurobiol* 40(3):224–235.
37. Carmeliet P, Jain RK (2011) Molecular mechanisms and clinical applications of angiogenesis. *Nature* 473(7347):298–307.
38. Nakatsu MN, Hughes CC (2008) An optimized three-dimensional in vitro model for the analysis of angiogenesis. *Methods Enzymol* 443:65–82.
39. Weinmann O, et al. (2006) Intrathecally infused antibodies against Nogo-A penetrate the CNS and downregulate the endogenous neurite growth inhibitor Nogo-A. *Mol Cell Neurosci* 32(1-2):161–173.
40. Hou T, et al. (2010) Nogo-A expresses on neural stem cell surface. *Int J Neurosci* 120(3): 201–205.
41. Dodd DA, et al. (2005) Nogo-A, -B, and -C are found on the cell surface and interact together in many different cell types. *J Biol Chem* 280(13):12494–12502.
42. Zagrebelsky M, Schweigreiter R, Bandtlow CE, Schwab ME, Korte M (2010) Nogo-A stabilizes the architecture of hippocampal neurons. *J Neurosci* 30(40):13220–13234.
43. Yiu G, He Z (2006) Glial inhibition of CNS axon regeneration. *Nat Rev Neurosci* 7(8): 617–627.
44. Niederöst B, Oertle T, Fritsche J, McKinney RA, Bandtlow CE (2002) Nogo-A and myelin-associated glycoprotein mediate neurite growth inhibition by antagonistic regulation of RhoA and Rac1. *J Neurosci* 22(23):10368–10376.
45. Aromolaran AS, Albert AP, Large WA (2000) Evidence for myosin light chain kinase mediating noradrenaline-evoked cation current in rabbit portal vein myocytes. *J Physiol* 524(Pt 3):853–863.
46. Kovács M, Tóth J, Hetényi C, Málnási-Csizmadia A, Sellers JR (2004) Mechanism of blebbistatin inhibition of myosin II. *J Biol Chem* 279(34):35557–35563.
47. Blanco R, Gerhardt H (2013) VEGF and notch in tip and stalk cell selection. *Cold Spring Harb Perspect Med*, 10.1101/cshperspect.a006569.
48. Geudens I, Gerhardt H (2011) Coordinating cell behaviour during blood vessel formation. *Development* 138(21):4569–4583.
49. Potente M, Gerhardt H, Carmeliet P (2011) Basic and therapeutic aspects of angiogenesis. *Cell* 146(6):873–887.
50. Risau W (1997) Mechanisms of angiogenesis. *Nature* 386(6626):671–674.
51. Lee HS, Han J, Bai HJ, Kim KW (2009) Brain angiogenesis in developmental and pathological processes: Regulation, molecular and cellular communication at the neurovascular interface. *FEBS J* 276(17):4622–4635.
52. le Noble F, Klein C, Tintu A, Pries A, Buschmann I (2008) Neural guidance molecules, tip cells, and mechanical factors in vascular development. *Cardiovasc Res* 78(2): 232–241.
53. Suchting S, Bicknell R, Eichmann A (2006) Neuronal clues to vascular guidance. *Exp Cell Res* 312(5):668–675.
54. Fischer RS, Gardel M, Ma X, Adelstein RS, Waterman CM (2009) Local cortical tension by myosin II guides 3D endothelial cell branching. *Curr Biol* 19(3):260–265.
55. Myers KA, Applegate KT, Danuser G, Fischer RS, Waterman CM (2011) Distinct ECM mechanosensing pathways regulate microtubule dynamics to control endothelial cell branching morphogenesis. *J Cell Biol* 192(2):321–334.
56. Mammoto A, Mammoto T, Ingber DE (2008) Rho signaling and mechanical control of vascular development. *Curr Opin Hematol* 15(3):228–234.
57. Montani L, et al. (2009) Neuronal Nogo-A modulates growth cone motility via Rho-GTP/LIMK1/cofilin in the unlesioned adult nervous system. *J Biol Chem* 284(16): 10793–10807.
58. Wei YT, et al. (2010) Hyaluronic acid hydrogel modified with nogo-66 receptor antibody and poly-L-lysine to promote axon regrowth after spinal cord injury. *J Biomed Mater Res B Appl Biomater* 95(1):110–117.
59. Yu J, et al. (2009) Reticulon 4B (Nogo-B) is necessary for macrophage infiltration and tissue repair. *Proc Natl Acad Sci USA* 106(41):17511–17516.
60. Hu F, Strittmatter SM (2008) The N-terminal domain of Nogo-A inhibits cell adhesion and axonal outgrowth by an integrin-specific mechanism. *J Neurosci* 28(5):1262–1269.
61. Vogel V, Sheetz M (2006) Local force and geometry sensing regulate cell functions. *Nat Rev Mol Cell Biol* 7(4):265–275.
62. Lu X, et al. (2004) The netrin receptor UNC5B mediates guidance events controlling morphogenesis of the vascular system. *Nature* 432(7014):179–186.
63. Koch AW, et al. (2011) Robo4 maintains vessel integrity and inhibits angiogenesis by interacting with UNC5B. *Dev Cell* 20(1):33–46.
64. Sapieha P, et al. (2008) The succinate receptor GPR91 in neurons has a major role in retinal angiogenesis. *Nat Med* 14(10):1067–1076.
65. Arese M, Serini G, Bussolino F (2011) Nervous vascular parallels: Axon guidance and beyond. *Int J Dev Biol* 55(4-5):439–445.
66. Tsai SY, et al. (2007) Intrathecal treatment with anti-Nogo-A antibody improves functional recovery in adult rats after stroke. *Exp Brain Res* 182(2):261–266.
67. Tsai SY, Papadopoulos CM, Schwab ME, Kartje GL (2011) Delayed anti-nogo-a therapy improves function after chronic stroke in adult rats. *Stroke* 42(1):186–190.
68. Cheatwood JL, Emerick AJ, Schwab ME, Kartje GL (2008) Nogo-A expression after focal ischemic stroke in the adult rat. *Stroke* 39(7):2091–2098.
69. Joyal JS, et al. (2011) Ischemic neurons prevent vascular regeneration of neural tissue by secreting semaphorin 3A. *Blood* 117(22):6024–6035.
70. Fukushima Y, et al. (2011) Sema3E-PlexinD1 signaling selectively suppresses disoriented angiogenesis in ischemic retinopathy in mice. *J Clin Invest* 121(5): 1974–1985.
71. Liao XX, et al. (2011) The expression patterns of Nogo-A, myelin associated glycoprotein and oligodendrocyte myelin glycoprotein in the retina after ocular hypertension: The expression of myelin proteins in the retina in glaucoma. *Neurochem Res* 36(11):1955–1961.
72. Kuhlmann T, et al. (2008) Nogo-a expression in glial CNS tumors: A tool to differentiate between oligodendrogliomas and other gliomas? *Am J Surg Pathol* 32(10):1444–1453.
73. Xiong NX, Zhao HY, Zhang FC, He ZQ (2007) Negative correlation of Nogo-A with the malignancy of oligodendroglial tumor. *Neurosci Bull* 23(1):41–45.
74. Cheung HC, et al. (2009) Splicing factors PTBP1 and PTBP2 promote proliferation and migration of glioma cell lines. *Brain* 132(Pt 8):2277–2288.